Manuscript Click here to view linked References

Dynamic characteristics of a curved steel-concrete composite cable-stayed bridge and effects of different design choices

Bruno Briseghella[a], Guanzhe Fa[b], Angelo Aloisio[c,*], Dag Pasca[d], Leqia He[a], Luigi Fenu[e], Carmelo Gentile[f]

[a] Sustainable and Innovative Bridge Engineering Research Center, College of Civil Engineering, Fuzhou University, China;
[b] Sustainable and Innovative Bridge Engineering Research Center, College of Civil Engineering, Fuzhou University, China;
[c] Department of Civil, Construction-Architectural and Environmental Engineering, University of L'Aquila, Italy;
[d] Norsk Treteknisk Institutt (Norwegian Institute of Wood Technology), Børrestuveien 3, 0373 Oslo, Norway.
[e] Department of Civil and Environmental Engineering and Architecture, University of Cagliari, Cagliari, Italy.
[f] Department of Architecture, Built environment and Construction engineering (DABC), Politecnico di Milano, Piazza Leonardo da Vinci 32, 20133 Milan Italy.

ARTICLE HISTORY
Compiled September 10, 2021

ABSTRACT
The paper presents and discusses the dynamic response of a curved cable-stayed bridge in Venice (Italy). Two distinct experimental campaigns in 2010 and 2011 led to identifying the bridge dynamic characteristics in operational conditions. The dynamic identification included the characterization of both the deck and cables response. The authors developed a highly refined finite element (FE) model of the bridge, mirroring up to twelve experimental modes. An updating procedure drove the estimate of the optimum parameters associated with the lowest discrepancy with the experimental modal parameters. The calibrated model was the base of a parametric analysis on the effects of the deck curvature, cables arrangement and tower cross-section inertia on the bridge dynamics. Specifically, the authors developed fourteen FE models of the bridge distinguished by the lack and different arrangement of the stay cables, the increasing value of the deck curvature and the tower inertia. The analysis intends to quantify the impact of the design choices of cable-stayed bridges on the modal parameters.

KEYWORDS
cable-stayed bridge; operational modal analysis; finite element modelling; sensitivity-based model updating; structural health monitoring.

1. Introduction

Cable-stayed bridges play a vital role in transportation systems [1]. Particularly in the last decade, cable-stayed bridges were built in unique styles due to structural and aesthetics requirements [2, 3, 4]. Examples include the bridge investigated in this paper, the bridge of Porto Marghera in Venice (Italy) [5, 6, 7]. Almost all existing cable-stayed bridges are straight, while just a few have curved decks. Examples of known curved cable-stayed bridges are the Rhine bridge near Schaffhausen in Switzerland [8], the Safti Link bridge in Singapore [9], the twin bridges close to the Milan-Malpensa airport [10], the Katsushika bridge in Japan [11], the Térénez bridge in France [12], the Yabegawa River Bridge [13] and the Ponte del Mare bridge in Pescara (Italy) [14, 6]. The peculiar structural architecture of curved cable-stayed bridges adds significant difficulties in accurate structural analysis during the design stage and assessing the "as-built" behaviour [15, 16]. The deck curvature may determine different effects on the bridge dynamics compared to a straight structure [17, 18]. Accordingly, all the mentioned bridges have been the object of dynamic testing to validate and refine structural models. The chief reason for choosing a curved structure is to accommodate the bridge to the existing urban or environmental layout. Not secondarily, the curvature provides generally appreciated aesthetic peculiarities [19].

In this paper, the authors present the model of a cable-stayed bridge in Porto Marghera. Model updating methods are used to calibrate a mathematical model, frequently a discretized FE model, with the experimental data [20]. The estimate of the optimum model is sensitive to multiple uncertainties related to the model's limitations, measurement and processing error, the number of modal components or time histories, and the metric used to evaluate the agreement with experimental data. The need for accurate model updating methods originates from several applications, like reliability analyses, structural health monitoring and structural control [21]. The updating algorithm based on the modal features or response time history often descend from solving a weighted least-squares problem. Conventional optimization procedures determine the optimal values of the structural parameters that minimize the single weighted residuals metric. Nevertheless, the results of the optimization are affected by the values of the chosen weighting factors. Alternatively, the model updating problem has also been formulated in a multi-objective context [22], allowing the concurrent minimization of multiple metrics, eliminating the need for arbitrary weighting factors, balancing the relative importance of each metric in the overall measure of fit. In this research, the authors adopted an iterative updating method for the solution of the optimization problem using the SAP2000-Matlab interaction [23].

In the last decade, dynamic identification and FE model updating have become a standard practice in structural engineering [24]. Still, the peculiarity of the considered structure, which entailed developing a highly-refined FE model, represents the value and originality of this research. A few studies focused on the dynamic identification of curved cable-stayed bridges due to the small number of these structural typologies. Additionally, this research transcends the limits of a case study by presenting an extensive parametric analysis on on the variation of the bridge dynamic characteristics induced by different design choices, such as the presence and arrangement of the stay cables, the deck curvature [25, 26] and the tower cross-section inertia [27, 28].
Specifically, the paper examines the dynamic characteristics of bridges similar to the real one but characterized by different geometric configurations. The differences are related to cables arrangement, deck curvature and cross-section of the tower: for each numerical simulation, the effect on the bridge dynamic characteristics is presented and discussed.
The paper has three main parts. In the first, there is the bridge description and the results of dynamic identification (Sec.2-4). The second part deals with the FE model updating (Sec.5-6). The third part discusses the results of the parametric analysis (Sec.7-8).

2. Case study

The bridge's construction was required to cross the West Industrial Canal in the Porto Marghera basin and complete the road connection between the national highway and the port areas [29]. The bridge is characterized by an inclined L-shape prestressed concrete tower, a single set of cables with a spatial arrangement and a curved steel-concrete composite deck [7].

2.1. Bridge description

The Porto Marghera bridge, connecting the city of Mestre to the Commercial Harbor of Venice-Marghera, Italy (Fig.1-2), has a total length of 387m, divided into six spans (42m+105m+126m+30+42m+42m). The first spans present a straight alignment, and the others a curved one with a 175m radius. Fig.3 shows the plan, elevation and typical cross-sections of the deck. The two main spans of the bridge exhibit a cable-stayed structure with the stays



(a) (b)

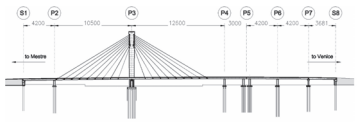
Figure 1. View of the Porto Marghera Bridge before (a) and after (b) being completed.

organized on a single plane, connected by the cross-section centre. The bridge has two traffic lanes and pedestrian walkways with a 23.70m total width. The structural arrangement of the deck consists of a composite concrete-steel continuous girder covering all six spans. There are two main cross-sections of the deck, depicted in Fig.3. The first one, adopted by the end-spans, consists of four double-T steel girders, while the second one, by the central spans, consists of two outer double-T steel girders and one central girder with a box section, see Fig.2. Transverse crossbeams made by double-T beams spaced every 5.25m stiffen the girder. Steel girders and crossbeams have a 1.90m height and are connected to a cast-in-place concrete slab with a 25-27 cm thickness. The cast-in-place prestressed concrete inclined tower represents the bridge landmark and played a determining role in the conceptual and executive design of the bridge. The tower has 75m approximate height, and a triangular cross-section characterizes its geometric layout. The cross-section base enlarges upward to provide a more suitable anchorage for the stays. The tower prestressing aimed at reducing the dead loads eccentricity due to the curved deck layout. Despite the classic static scheme conception, typical of cable-stayed bridges with central tower, numerous elements present a considerable architectonic impact and originality: the curvilinear layout of the suspended deck, the suspension scheme with a central curtain of stays and the inclined tower with variable section. The remarkable size of the deck made in the open profile (23.7m) and the mentioned bridge singularities supported the dynamic identification of the bridge for the experimental assessment of its dynamic response.

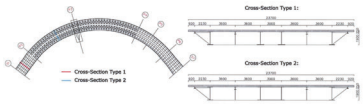


(a) (b)

Figure 2. (a) Typical cross section of the bridge during construction (concrete slab not cast yet) and (b) the layout of the prestressing cables within the tower.



(a) Elevation.



(b) Plan and typical cross sections.

Figure 3. Schematic plan view of the deck and typical cross-sections (dimensions in cm in (a) and mm in (b)).

3. Operational Modal Analysis of the bridge

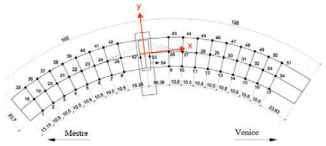
The Laboratory of Vibrations and Dynamic Monitoring of Structures of Politecnico di Milano carried out the dynamic identification of the Porto Marghera bridge in two experimental campaigns. The twos carried out in Autumn 2010 and Spring 2010 had the twofold objectives of verifying the correspondence with the findings from the first investigation in 2006 and assessing the possible effects temperature differences between the experimental tests in 2010 and 2011 or damage on the structure's dynamic response [30, 31]. The two studies identified the modal parameters of the bridge and the natural frequencies and damping of the cable stays. The experimental modal analysis of the bridge was carried out using the Frequency Domain Decomposition [22]. The natural frequencies of the stays derived from the direct inspection of the auto spectra of the recorded signals [32].

3.1. Experimental setup

Ambient vibration tests were carried out using a 16-channel data acquisition system with 14 uniaxial piezoelectric accelerometers (WR model 731A), see Fig.4. Each sensor was connected to a power unit/amplifier providing the needed power supply and selective filtering. The sampling frequency was 200Hz. The duration of each acquisition was 60 minutes.



(a) (b)

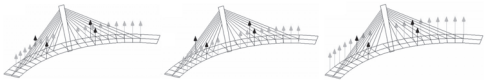


(c) Layout 2010/2011

Figure 4. (a) Piezoelectric accelerometer WR 731A with power supply WR P31. (b)-(c) Plan view of the experimental layouts in 2010/2011.

Three sensors configurations were adopted. In the first, 15 vertical sensors were along the inner edge of the sidewalk on the inside curve. In the second, 17 vertical sensors were along the central line and three horizontal sensors on the antenna section at a 13.5m height to the deck extrados. In the third configurations, 16 vertical sensors were positioned along the inner edge of the sidewalk on the outside curve. The total number of measurement points was 54 in 2010. The total number of measurement points reduced to 51 in 2011 by removing the sensors installed on the antenna (positions No 52, 53, and 54). The results of the 2010 investigation

returned negligible values of the modal displacements in the considered three measurement points.



(a) Setup 1 (2010/2011) (b) Setup 2 (2010/2011) (c) Setup 3 (2010/2011)

Figure 5. View of the setups with indication of the measurement axes. The black arrows indicate the reference accelerometers, the gray arrows the moving ones.

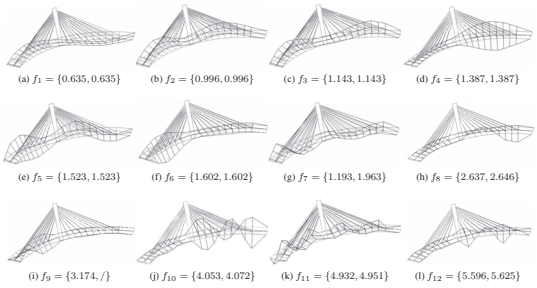
3.2. Experimental results

The analysis of the signals led to the identification of 12 modes in 0-6 Hz range. In 2010 and 2011, the bridge response was acquired under vehicular traffic, possibly magnifying some modal responses compared to others. Tab.1 compares the modal parameters identified in 2010 and 2011. Fig.6 shows a representation of the mode shapes. The pictures include the tower and the stays, although the displayed modal deformations refer to the sole deck. Except for the first bending modes, most of them are torsional or bending-torsional. The geometric configuration of the structure and the excitation condition, characterized by prevalent transit of heavy vehicles rarely engaging the two lanes simultaneously, significantly affected the modal parameters. Likely, the bending-torsional modes disavow the assumption of transversal non-deformability of the profile. Still, this type of behaviour is consistent with the open-profile section with a high aspect ratio.

Table 1. Comparison between the modal parameters estimated from experimental campaigns in 2010 and 2011.

No	f_{2010}[Hz]	f_{2011}[Hz]	$\frac{f_{2010}-f_{2011}}{f_{2010}}$ [%]	$MAC_{2010-2011}$
1	0.635	0.635	0.00	0.988
2	0.996	0.996	0.00	0.980
3	1.143	1.143	0.00	0.958
4	1.387	1.387	0.00	0.998
5	1.523	1.523	0.00	0.982
6	1.602	1.602	0.00	0.990
7	1.953	1.963	-0.51	0.988
8	2.637	2.646	-0.34	0.983
9	3.174	/	/	/
10	4.053	4.072	-0.47	0.954
11	4.932	4.951	-0.39	0.836
12	5.596	5.625	-0.52	0.835

The curvilinear configuration of the deck determines the three-dimensional nature of all modes. However, the maximum ratio between the transverse and vertical modal amplitudes is about 0.20 (mode No 9). This observation proves the prevalence of the vertical component in the detected modes. In particular, the ratio between the maximum amplitudes in the transversal and vertical direction is higher than 0.10 for modes No 2 and 5. Similar behaviour with a minor coupling between the vertical and transverse displacements of the deck emerged in the twin cable-stayed bridges with the curvilinear axis of the Milan-Malpensa airport. The tower does not participate significantly in the bridge dynamics. Specifically, modes No 1,5,6,7 exhibit notable longitudinal motion of the antenna. Modes No 2,15 present both the



(a) $f_1 = \{0.635, 0.635\}$ (b) $f_2 = \{0.996, 0.996\}$ (c) $f_3 = \{1.143, 1.143\}$ (d) $f_4 = \{1.387, 1.387\}$

(e) $f_5 = \{1.523, 1.523\}$ (f) $f_6 = \{1.602, 1.602\}$ (g) $f_7 = \{1.193, 1.963\}$ (h) $f_8 = \{2.637, 2.646\}$

(i) $f_9 = \{3.174, /\}$ (j) $f_{10} = \{4.053, 4.072\}$ (k) $f_{11} = \{4.932, 4.951\}$ (l) $f_{12} = \{5.596, 5.625\}$

Figure 6. Experimental mode shapes detected in the three experimental campaigns. The sub captions indicate the natural frequencies of each mode corresponding to the dynamic identifications carried out 2010 and 2011 respectively.

longitudinal and transverse deformation of the tower. The modal deformations associated with modal order higher than 11 are not consistent with the assumption of transversal non-deformability of the profile.

The Modal Assurance Criterion (MAC, [33]) values of the corresponding modes are generally very high ($\geq$0.94) and prove the substantial invariance of the mode shapes between the two experimental observations. The natural frequencies identified in 2010 and 2011 are almost indistinguishable. The quantitative comparison between the modal parameters unveils the substantial invariance of the natural frequencies of all the analogous modes, with percentage deviations less than 1%, in the range 0.15%-0.52%. The authors did not notice evident dependence of the modal parameters on the temperature [34]. Additionally, there is an evident invariance of the mode shapes between the two experimental observations: the MAC values are higher than 0.95.

4. Dynamic characterization of the cables

The dynamic behaviour of the stays was also investigated. Each cable stay was instrumented with a single sensor, placed at approximately 9.0m to the road surface. In particular, two measurement arrangements were adopted, shown in Fig.7. Firstly the response of stays on the Mestre side was acquired, while in a second step, that of the cable stays on the Venice side. Even in these setups, the sampling frequency was equal to 200 Hz, and the duration of the time signal was 3000 s.

Fig.8 compares the natural frequencies of the 18 stay cables identified in 2010 and 2011. Each figure reports the results of two symmetric stay cables, following the numbering in Fig.7. Fig.8 plots the natural frequencies and interpolating line n-f_n, where n is the mode order, and f_n is the associated natural frequency. The deviation between interpolating lines

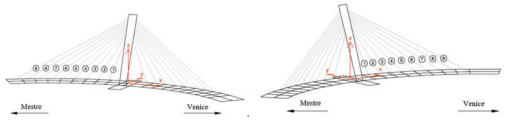


Figure 7. Numbering of the stay cables.

and the experimental natural frequency provides a simplified measure of the discrepancy to the most elementary mechanical model of a cable, represented by a plane elastic string under small deformations. The non-proportionality between natural frequencies and the mode order entails the adoption of more accurate mechanical models. Additionally, the considered elementary mechanical model could be used for the indirect estimate of the force in each cable. However, the derivation of the cable force from the cable dynamics requires dedicated efforts and it is not the object of this research paper.

Table 2. Fundamental natural frequencies of the stay cables estimated in 2010 and 2011. The first nine values refer to the Mestre side, the second nine to the Venice side.

	First natural frequency [Hz]	
Stay cable no.	2010	2011
1	1.250	1.230
2	1.211	1.211
3	1.621	1.621
4	1.543	1.543
5	1.387	1.387
6	1.289	1.289
7	1.250	1.250
8	1.113	1.094
9	0.977	0.977
1	1.445	1.406
2	1.309	1.289
3	1.641	1.641
4	1.563	1.563
5	1.426	1.406
6	1.328	1.328
7	1.230	1.230
8	1.094	1.113
9	0.938	0.938

The fundamental frequencies of the stays on the Mestre side display a minor difference to the symmetric stays on the Venice side, except for the two shorter ones, whose frequencies differ by 15.6% and 8.1%, respectively. The damping values are very low (always less than 1%), possibly due to the low excitation level [35]. There is a deviation from the elementary string model in the two shorter cables, while the discrepancy progressively reduces as the cable length raises.
The comparison between the results obtained in 2010 and 2011 confirmed two observations. (i) In the shorter stays, there is a significant deviation of the interpolating lines n-f_n from the theoretical model of a vibrating string. (ii) In the other stays, the fixed-fixed vibrating string's deviations progressively reduce as the length of the suspension elements increases. The fundamental frequencies on the Mestre side are practically invariant, as evidenced by Fig.8. In the shorter stays, there is a very slight decrement of the natural frequency between

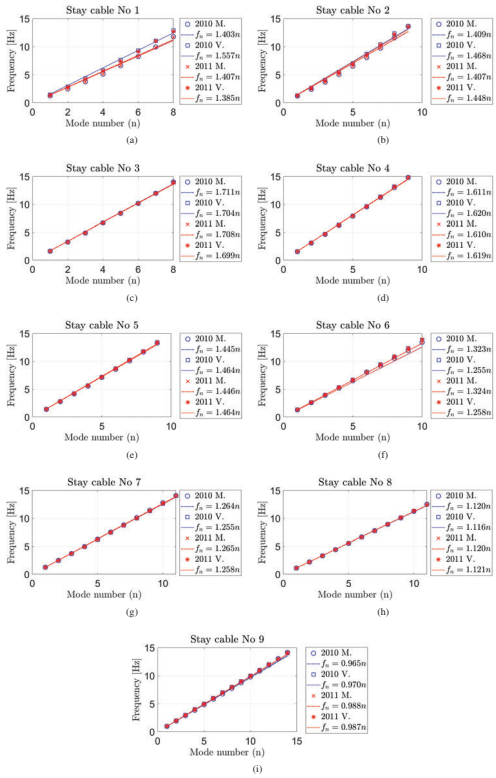


Figure 8. Natural frequencies of the nine stay cables on the Mestre side and their correlation with the mode number.

2010 and 2011. Conversely, the stays on the Venice side manifest a peculiar phenomenon. There is a decrease in the natural frequencies of the shorter stays and an increase in the natural frequencies of the longer ones. The substantial invariance observed in the Mestre side stays possibly prove that this variation does not depend on thermal effects. However, this phenomenon, observed in 2011, has not manifested in recent investigations.

5. Finite Element modelling

A refined CAD model reproduced the in-plane deck curvature and its transverse slope, different in each bridge segment to a maximum of 4.5%. The CAD model was subsequently exported into MIDAS and, in a second step, to SAP2000 to generate the FE model of the bridge. Three and four-nodes shell elements reproduced the concrete slab, while solid elements the tower. Two-nodes 3D beam elements modelled the concrete piers. The weight per unit volume and the Poisson's ratio of the concrete were assumed to be 25.0 kN/m^3 and 0.2, respectively. An additional weight equal to 1 kN/m^2 represented the deck slab, including the asphalt pavement and walkways. Two-nodes 3D beam elements modelled steel stringers, transverse cross-beams and bracings of the deck. The Young's modulus and steel weight was assumed to be 205 GPa and 785 kN/m^3. Rigid links, without mass, connected the concrete slab and the grid of steel stringers and transverse cross-beams. Additionally, rigid links reproduced geometrical offsets between the structural members and strut-and-tie bracings of the deck. 3D truss elements modelled the stays. The boundary conditions between piers and the foundation were assumed as fixed. The deck constraints were modelled by introducing translational beam end-releases between the transverse frame elements and the lower piles according to the construction drawing. The resulting FE model in Fig.9 has 8014 nodes and 6600 elements (namely 2946 beams, 18 trusses, and 3636 solid elements). The FE model is linear and, consequently, does not represent possible geometrical or mechanical nonlinear phenomena. Most of the modelling uncertainties are related to the Young's modulus of the

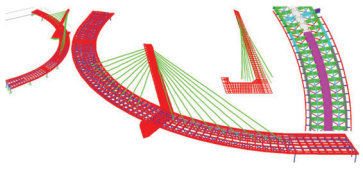
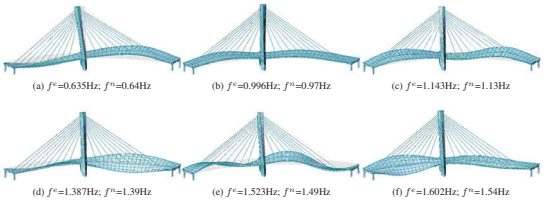


Figure 9. An a-priori FE model of the Porto Marghera bridge developed in SAP2000.

concrete (E_c). Consequently, the authors developed preliminary dynamic analyses to investigate the agreement between experimental and numerical modal parameters. The concrete Young's modulus ranged from 34 to 42GPa. The authors estimated separately the concrete Young's modulus of the structure ($E_{c,d}$) and substructure ($E_{c,p}$). A first manual tuning provided the following values of $E_{c,d}$ = 40.0 GPa, $E_{c,p}$= 36.0 GPa. The accord between the numerical and experimental data is very satisfactory and yields minor errors. Fig.10 shows a few selected mode shapes of the FE model.

The FE model in Fig.9 refers to the bridge condition in 2010/2011. Therefore, the sole outcomes of the 2010 dynamic identification were used for model updating. A sensitivity analysis



(a) f^e=0.635Hz; f^n=0.64Hz (b) f^e=0.996Hz; f^n=0.97Hz (c) f^e=1.143Hz; f^n=1.13Hz

(d) f^e=1.387Hz; f^n=1.39Hz (e) f^e=1.523Hz; f^n=1.49Hz (f) f^e=1.602Hz; f^n=1.54Hz

Figure 10. Representation of a few selected numerical modes. f^e and f^n in the sub-captions indicate the experimental and numerical natural frequencies.

of the thirteen modal frequencies to the Young's modulus of steel and concrete of each structural component, E_s and E_c respectively, revealed the significant sensitivity of the natural frequencies to the Young's modulus of the stringers crossbeams, tower, slab and pedestrian overlays. Therefore, the updating focused on the mentioned structural elements, distinguished by higher sensitivity to the Young's modulus.

5.1. Model updating

The authors implemented a model updating algorithms used for the mutual validation of the optimization results. The method, labelled iterative method, does not express the functional dependence of the objective function to the modelling parameters and generates an iterative sampling of the space of the parameters. The following subsection briefly reviews the mathematical details of the method.

5.1.1. Iterative method

A sensitivity iterative algorithm based on the trust-region reflective algorithm with the upper and lower bounds being provided [36] is implemented for the model updating. The modal parameters in terms of natural frequencies and mode shapes are directly included in the objective function [37]. In detail, the authors solved the following nonlinear least-squares problem:

$$\hat{\boldsymbol{\theta}} = \arg\min_{\boldsymbol{\theta}} J(\boldsymbol{\theta}) = \arg\min_{\boldsymbol{\theta}} \boldsymbol{\epsilon}_z(\boldsymbol{\theta})^T \boldsymbol{W}_e \boldsymbol{\epsilon}_z(\boldsymbol{\theta}) = \arg\min_{\boldsymbol{\theta}} \sum_i w_{e,i} \left(\epsilon_{z,i}(\boldsymbol{\theta})\right)^2 \quad (1)$$

where $\epsilon_{z,i}$ denotes the residuals between the experimental and numerical modal data z. The residuals associated with the undamped eigenvalue $z = \lambda$, where $\lambda_i = (2\pi f_i)^2$, are

$$\epsilon_{\lambda_i}(\boldsymbol{\theta}) = \frac{\lambda_i(\boldsymbol{\theta}) - \tilde{\lambda}_i}{\tilde{\lambda}_i} | i \in \{1 - n\} \quad (2)$$

where the upper tilde denotes the experimental values and f stands for the natural frequency. The residuals associated with the mode shapes are:

$$\boldsymbol{\epsilon}_{\boldsymbol{\phi}_i}(\boldsymbol{\theta}) = \frac{\boldsymbol{\phi}(\boldsymbol{\theta}) - \tilde{\boldsymbol{\phi}}_i}{\|\tilde{\boldsymbol{\phi}}_i\|} | i \in \{1 - n\} \quad (3)$$

where both the numerical and experimental mode shape vectors ($\boldsymbol{\phi}_i$ and $\tilde{\boldsymbol{\phi}}_i$) are normalized to the maximum unity and only the real parts are considered. The authors assumed the weighting matrix, $\boldsymbol{W}_e$, equal to the identity matrix, to achieve an equal balance between all contributions to the residuals. The aforementioned sensitivity-based model updating was implemented into an interactive procedure based on MATLAB and SAP2000.

6. Results

The experimental modal parameters estimated in 2010 are the target of FE updating. The reference values of the Young's modulus of steel (E_s) and concrete (E_c) are $E_{s,deck,0}$=205GPa $E_{s,bracing,0}$=205GPa, $E_{c,slab,0}$=33GPa and $E_{c,tower,0}$=36GPa. The solutions of the iterative method were $E_{s,deck,I}$=216GPa $E_{s,bracing,I}$=218GPa and $E_{c,slab,I}$=33.74GPa $E_{c,tower,I}$=41.67GPa. Tab.3 lists the values of the Young's modulus obtained from the two algorithms. The w_f and w_z were set equal to 2 and 4, respectively. Tab.4

Table 3. Results of the optimization methods in GPa.

Parameter	Reference	Iterative method (I.M)
$E_{s,deck}$	205.00	216.00
$E_{s,bracing}$	205.00	218.00
$E_{c,slab}$	33.00	33.74
$E_{c,tower}$	36.00	41.67

shows the final FE-updated modal frequencies. The differences between the measured and FE natural frequencies range from 0% in the first mode to -10.7% in the fifth mode. In total, the FE model mirrors the first twelve experimental modes between 0.62 Hz and 5.46 Hz. The authors neglected the first, second and third modes because they are purely translational. Tab.4 reviews the results of the updating.

Table 4. Comparison between the experimental and numerical modal parameters. f_e denotes the experimental natural frequencies estimated in 2010, the subscripts i and I designate the values associated with the initial FE model and the FE model updated using the Iterative method. The letters V, M, and T indicate the prevalent mode nature, Bending Mixed or Torsional respectively.

No	Mode	f_e[Hz]	f_i[Hz]	$\frac{f_i - f_e}{f_e}$[%]	MAC$_i$	f_I[Hz]	$\frac{f_I - f_e}{f_e}$[%]	MAC$_I$
1	V1	0.635	0.62	-2.36	0.96	0.64	0.79	0.96
2	V2	0.996	0.91	-8.63	0.96	0.97	-2.61	0.95
3	B3	1.143	1.10	-3.76	0.98	1.13	-1.14	0.98
4	T1	1.387	1.38	-0.50	0.89	1.39	0.22	0.98
5	M1	1.523	1.44	-5.45	0.96	1.49	-2.17	0.97
6	T2	1.602	1.50	-6.37	0.88	1.54	-3.87	0.85
7	V4	1.953	1.95	-0.15	0.97	2.00	2.41	0.87
8	T3	2.637	2.53	-4.06	0.84	2.63	-0.27	0.94
9	T4	3.174	2.83	-10.84	0.93	2.98	-6.11	0.93
10	T5	4.053	3.95	-2.54	0.95	4.10	1.16	0.94
11	T6	4.932	4.77	-3.28	0.91	4.97	0.77	0.92
12	T7	5.596	5.46	-2.43	0.95	5.69	1.68	0.95

7. Effect of the bridge in-plane curvature and the cables presence and arrangement on the Porto Marghera bridge

This section highlights the effect of the design choices on the dynamics of the Porto Marghera bridge, namely the presence and configuration of the stay-cables and the in-plane curvature of the deck. Three categories of FE models are selected, distinguished by the same spatial development (42m+105m+126m+30m+42m+42m), geometric and material details of the updated FE model obtained from the iterative optimization algorithm. The first category, depicted in Fig.11(a)-(b), represents the Porto Marghera bridge without the stay-cables and increasing in-plane curvature of the deck. Specifically, the following values of the radii of curvature were selected: 123m, 175m (the Porto Marghera bridge), 400m and ∞ (straight deck). The second class of FE models, represented in Fig.11(c)-(d), reproduces the Porto Marghera bridge with its actual stay-cables configuration, arranged in a single plane, passing through the axis line of the bridge and the connection zone of the cables. Analogously to the first class, they developed four FE models with the following in-plane radii of curvature of the deck: 123m, 175m, 400m and ∞. The third class, depicted in Fig.11(e)-(f), models the Porto Marghera bridge with the stay-cables arranged on two planes. Differently from the first and second class, the curvature values are 175m and ∞. This model had the sole purpose of estimating the effect of the stay-cables arranged in two planes, passing through the edge lines of the bridge and the connection zone of the cables. The sole FE model with a single curtain of stay cables

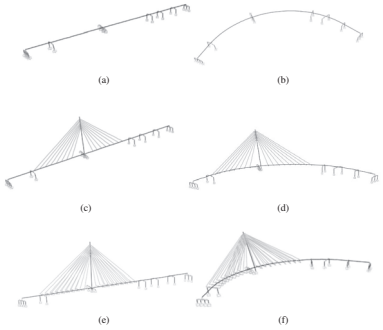


Figure 11. Illustration of the six FE models characterized by straight (a),(c),(e) and curved deck (b),(d),(f). Specifically, (a)-(b) with no stay cables, (c)-(d) with a single curtain of stay cables and (e)-(f) with a double curtain of stay cables.

and radius of curvature equal to 175m represents the actual Porto Marghera bridge. The other nine FE models originated from the main one by modifying or eliminating the stay-cables or altering the in-plane curvature of the deck.

The natural frequency and the predominant mode shape typology express the comparison between the models. The authors recognised four categories of mode shapes, based on the

Table 5. Comparison between the modal parameters of the models in Fig.11. T stands for torsional mode; V vertical mode; M mixed of torsional and vertical modes; TP transverse bending of tower.

	Without stay cables				Single curtain of stay cables				Double curtain of stay cables			
	Straight		Curved (R=175m)		Straight		Curved (R=175m)		Straight		Curved (R=175m)	
No.	f [Hz]	Mode	f [Hz]	Mode	f [Hz]	Mode	f [Hz]	Mode	f [Hz]	Mode	f [Hz]	Mode
1	0.61	V	0.51	V	0.82	V	0.64	TP	0.62	TP	0.49	TP
2	0.76	V	0.74	V	1.35	V	0.97	V	0.89	V	0.89	V
3	1.62	V	1.40	V	1.96	V	1.13	V	1.70	V	1.81	V
4	2.02	V	2.01	V	2.24	V	1.39	V	2.22	V	2.30	V
5	3.13	V	2.72	V	2.25	TP	1.49	M	2.44	V	2.80	V
6	3.44	T	3.19	T	2.45	V	1.54	V	2.77	V	3.05	M
7	4.01	T	3.36	M	3.32	V	2.00	M	3.41	T	3.14	M
8	4.06	V	3.81	V	3.42	T	2.63	T	3.48	V	3.17	M
9	4.63	T	3.96	M	3.98	T	2.98	M	3.96	T	3.39	M
10	5.26	V	4.09	V	4.01	V	4.10	V	4.20	V	3.48	V
11	5.47	V	4.44	T	4.20	V	4.97	T	4.36	V	3.91	T
12	5.62	T	4.45	V	4.63	T	5.69	M	4.75	T	4.22	V

prevalence of the modal components, labelled V, T, M, VP, TP. The V and T labels indicate the modes with prevalent vertical bending or torsion of the deck. The M label denotes the modes with a mix of vertical and torsional components, i.e. asymmetric bending. The TP and VP indicate the torsional and bending modes of the tower. Tab.5 lists selected results of the parametric analysis. It shows the natural frequency and the mode typologies of the three FE classes referred to the bridges with radii of curvature equal to 175m and ∞. Parallelly, Fig.12 represents all the results of the parametric analysis associated with the ten FE models. The three different colours, black, red and blue, identify the results of the three classes. A different pattern of the line designates the diverse choice of the deck curvature, while the different markers indicate the mode typologies.

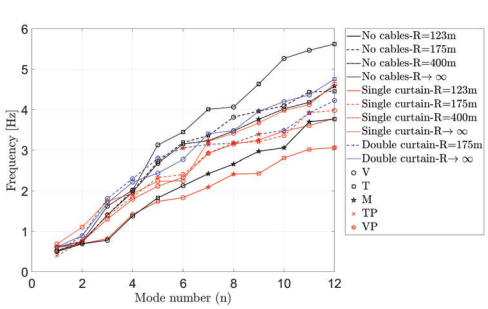


Figure 12. First natural frequencies of the considered 10 FE models. V stands for Vertical bending mode, T for torsional mode, M for mixed flexo-torsional, VP for the vertical bending of the tower, TP for the torsional mode of the tower.

The analysis of the results in Fig.12 highlights the following aspects.

- **Effect of the in-plane curvature of the deck**. The increment of the deck curvature causes the reduction of the natural frequencies of all the considered modes in the three FE classes. Even the mode of the tower, which should be less dependent on the deck curvature, exhibits a frequency reduction due to the deck curvature. This aspect proves that all the modes do not exhibit a pure deformation of each structural component, separately, e.g. the deck, the tower, the cables. Each mode presents a prevalence of deformation, useful for engineering classifications, but all modes are global. All modes can exhibit a localization of deformation, as remarked in the previous paragraphs.
  The increment of the in-plane curvature causes an apparent stiffness reduction of the deck. The eccentricity of the loads in the curved deck causes an additional torsion, which maximizes the inertial effects and reduces the natural frequencies. The inertial effect due to the deck curvature is partially compensated by the inclined tower, lessening eccentricity.
  Interestingly, the natural frequencies in the FE element models without and with the stay-cables reduce between the straight to the curved deck. Specifically, the average differences between the straight and curved deck in the first two FE classes are -0.49Hz and -0.33Hz, respectively. There is an approximate 0.15Hz frequency increment due to the balancing effect of the inclined tower. On average, the differences between natural frequencies are more significant in the torsional modes, up to 0.67Hz, and in the higher modes, up to 1.17Hz. This aspect proves that the additional inertial effects due to the load eccentricity are the leading cause of the frequency reduction associated with the torsional modes.
- **Effect of the stay-cables arrangement.** The adoption of stay-cables arranged in two symmetric planes should reduce the torsional effects on the deck. The difference between the linear structures in the second and third FE classes are insignificant. The frequency variations are minor and of both signs. The straight bridge with a double curtain of stay cables exhibits an avarage 0.01Hz increment of the natural frequency, compared to the one with a single curtain of stay cables.
  The double arrangement of the stay cables reduces the torsional response of the deck, leading to a 0.13Hz average increment of the natural frequency of the torsional modes due to the higher torsional stiffness. However, the double curtain of stay cables causes a reduction of the natural frequency of the vertical bending modes averagely equal to -0.2Hz. This aspect may depend on the spatial eccentricity of the stay cables in the double-curtain configurations, which cause an additional inertial effect on the vertical bending response.
  Conversely, the effects of the double curtain of stay-cables are almost uniform in the curved deck cases. Accurately, the arrangement of the stay cables in two planes determines an average 0.24Hz increment of the natural frequencies. The curved deck with a single plane of stay cables maximizes the torsional effects of the load, especially in wide cross-sections. The double arrangement enhances the torsional stiffness of the deck, manifesting in a frequency increment of the torsional and bending modes. In the curved configuration, the load eccentricity maximizes the inertial effects of the load, partially compensated by a higher torsional stiffness of the cross-section and the inclined tower.

Fig.13,14 and 15 show the mode shapes of the three FE models classes, each with two radii of curvature, 175m and ∞. The representation of the mode shapes might be redundant, but it could be valuable to the reader in discerning the effects of curvature and the presence/arrangement of the stay cables on the mode shapes.

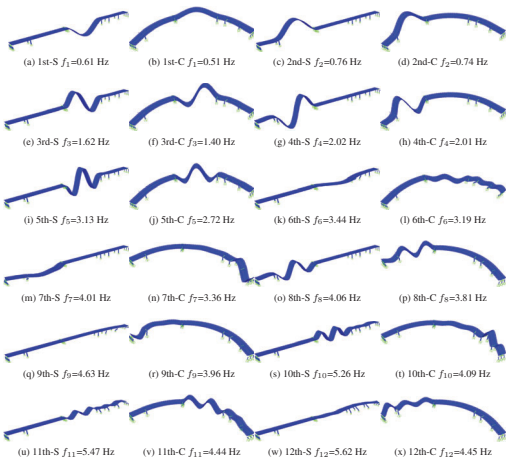
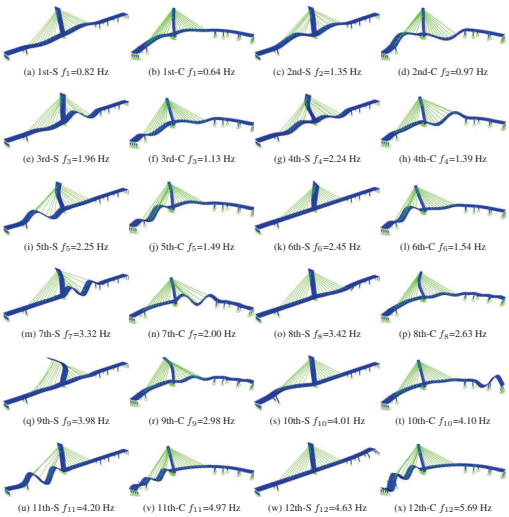


Figure 13. View of the mode shapes associated with the straight (S) and curved (C) models of Fig.11(a)-(b).



(a) 1st-S f_1=0.82 Hz (b) 1st-C f_1=0.64 Hz (c) 2nd-S f_2=1.35 Hz (d) 2nd-C f_2=0.97 Hz

(e) 3rd-S f_3=1.96 Hz (f) 3rd-C f_3=1.13 Hz (g) 4th-S f_4=2.24 Hz (h) 4th-C f_4=1.39 Hz

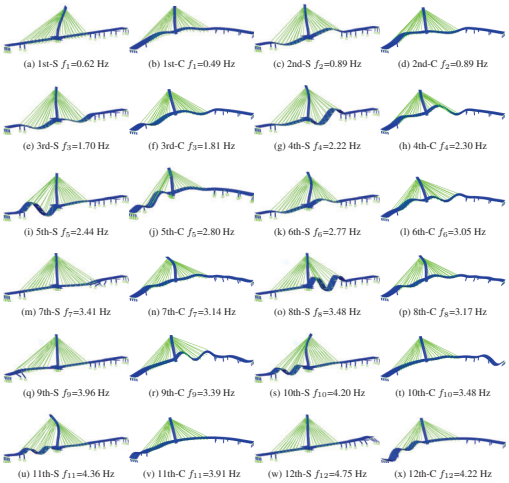
(i) 5th-S f_5=2.25 Hz (j) 5th-C f_5=1.49 Hz (k) 6th-S f_6=2.45 Hz (l) 6th-C f_6=1.54 Hz

(m) 7th-S f_7=3.32 Hz (n) 7th-C f_7=2.00 Hz (o) 8th-S f_8=3.42 Hz (p) 8th-C f_8=2.63 Hz

(q) 9th-S f_9=3.98 Hz (r) 9th-C f_9=2.98 Hz (s) 10th-S f_{10}=4.01 Hz (t) 10th-C f_{10}=4.10 Hz

(u) 11th-S f_{11}=4.20 Hz (v) 11th-C f_{11}=4.97 Hz (w) 12th-S f_{12}=4.63 Hz (x) 12th-C f_{12}=5.69 Hz

Figure 14. View of the mode shapes associated with the straight (S) and curved (C) models of Fig.11(c)-(d).



(a) 1st-S f_1=0.62 Hz (b) 1st-C f_1=0.49 Hz (c) 2nd-S f_2=0.89 Hz (d) 2nd-C f_2=0.89 Hz

(e) 3rd-S f_3=1.70 Hz (f) 3rd-C f_3=1.81 Hz (g) 4th-S f_4=2.22 Hz (h) 4th-C f_4=2.30 Hz

(i) 5th-S f_5=2.44 Hz (j) 5th-C f_5=2.80 Hz (k) 6th-S f_6=2.77 Hz (l) 6th-C f_6=3.05 Hz

(m) 7th-S f_7=3.41 Hz (n) 7th-C f_7=3.14 Hz (o) 8th-S f_8=3.48 Hz (p) 8th-C f_8=3.17 Hz

(q) 9th-S f_9=3.96 Hz (r) 9th-C f_9=3.39 Hz (s) 10th-S f_{10}=4.20 Hz (t) 10th-C f_{10}=3.48 Hz

(u) 11th-S f_{11}=4.36 Hz (v) 11th-C f_{11}=3.91 Hz (w) 12th-S f_{12}=4.75 Hz (x) 12th-C f_{12}=4.22 Hz

Figure 15. View of the mode shapes associated with the straight (S) and curved (C) models of Fig.11(e)-(f).

8. Effect of the tower cross-section inertia to the modal parameters

This section investigates the dynamic properties of the tower cross-section on the bridge dynamics. The authors fictitiously increased the tower stiffness by incrementing its cross-section inertia. They selected four arbitrary multiplication factors of the cross-section inertia: 1, 1.25,2 and 2.75. In this section, the authors modelled the Porto Marghera Bridge, distinguished by a 175m radius of curvature, with a double arrangement of stay cables. The arrangement of the stay-cables in two planes is associated with a more satisfactory dynamic performance due to higher natural frequencies. The authors wonder whether a stiffer tower can further enhance the benefits of a double curtain of stay cables. Tab.6 lists the natural frequencies and mode typologies of the considered four FE models with increasing inertia of the tower cross-section.

Table 6. Effect of the increasing cross-section inertia of the tower over the first natural frequencies. 1x, 2.25x, 2x and 2.75 indicate the multiplication factors of the tower cross-section inertia. TP, V, T and M designate the mode types: Torsional of the tower, Vertical bending, Torsional and Mixed bending-torsional respectively.

No.	Mode type	f [Hz] 1x	f [Hz] 1.25x	f [Hz] 2x	f [Hz] 2.75x
1	TP	0.491	0.526	0.583	0.636
2	V	0.887	0.961	0.991	1.016
3	V	1.809	1.881	1.888	1.891
4	V	2.299	2.457	2.472	2.479
5	V	2.800	3.025	3.073	3.089
6	M	3.050	3.209	3.262	3.299
7	M	3.139	3.381	3.383	3.383
8	M	3.169	3.499	3.722	3.727
9	M	3.393	3.737	3.819	3.819
10	V	3.483	3.820	4.199	4.200
11	T	3.914	4.198	4.363	4.363
12	V	4.223	4.363	4.396	4.687

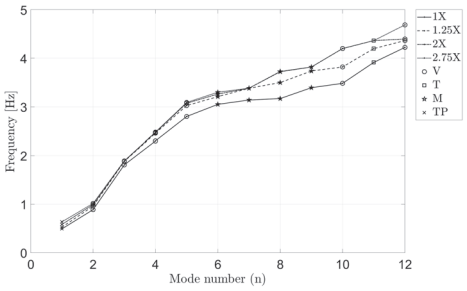


Figure 16. First natural frequencies of the FE model of the bridge with double curtain of stay cables and variable inertia of the tower. Specifically, 1X, 1.25X, 2X and 2.75X indicate the multiplication factors of the tower mass per unit of volume. V stands for Vertical bending mode, T for torsional mode, M for mixed bending-torsional, TP for the torsional mode of the tower.

Fig.16 shows the succession of the first twelve modes of the four FE models with the indication of the prevalent mode shapes. The modification of the tower cross-section affects all mode shapes. The experimental data and numerical analyses showed that the deformation of the tower is negligible in the modes with prevalent deformation of the deck. Two main aspects arise from this parametric analysis:

- The increment of the inertia causes the increment of the first torsional frequency of the tower. The average percentage increment of the natural frequencies of the deck are 6.7%, 9.7% and 11.2% in the models with 1.25, 2 and 2.75 multiplication factors, respectively (see Tab.6). The frequency increment is almost linearly proportional to the multiplication factors in the considered range of variation. The percentage slope of the interpolating line, correlating the percentage frequency increment and the multiplication factors, is 9.36%.
- Analogously, the effect of the increased inertia of the tower cross-section causes an evident reduction of the natural frequencies of the deck. The average percentage reduction of the deck natural frequencies are -6.8%, -8.6% and -10.10% in the models with 1.25, 2 and 2.75 multiplication factors, respectively (see Tab.6). The frequency increment is almost linearly proportional to the multiplication factors in the considered range of variation. Accurately, the percentage slope of the interpolating line, correlating the percentage frequency increment and the multiplication factors, is -2.02%.
- An increment of the rotational inertia of the tower affects all modes, not just the ones with a prevalent tower deformation. Though, the effects of the increasing inertia are more predominant in the torsional mode of the tower.

9. Conclusions

The authors presented the dynamic identification, model updating and parametric analysis of a curved cable-stayed bridge in Porto Marghera, Italy. The interpretation of the acceleration signals acquired in two experimental campaign (2010 and 2011) led to the identification of 13 modes in the range 0-9 Hz. Except for the first two bending modes, higher modes are torsional or bending-torsional. The satisfactory correlation between similar modal shapes proves their substantial invariance between the three experimental observations. The cables manifested a typical dynamic behaviour and relatively low damping values, less than 1%. Except for cables with shorter length, the detected natural frequencies reveal a dynamic behaviour corresponding to a vibrating string. Interestingly, the auto-spectra of the signals recorded on the stays show peaks in correspondence with the global structure's 6-7 global modes. This event suggests the possible application of the interferometry radar or vision-based techniques [38, 39] for the remote monitoring of the bridge dynamics [40].

In a second step, the authors developed a refined FE model of the deck characterized by 8014 nodes and 6600 elements. They successfully tuned the model to the experimental modal parameters using an iterative updating algorithms. The updated model reproduces the first twelve experimental modes identified in 2010 with high MAC and minor frequency discrepancies. Ultimately, the authors assessed the effects of the design choices on the bridge dynamics: the in-plane curvature of the deck, the presence and arrangement of the stay-cables in two or one plane and the cross-section inertia of the tower. The parametric analysis was based on thirteen FE models originated from the Porto Marghera one. Specifically, they developed three categories of FE models, distinguished by the same spatial development (42m+105m+126m+30m+42m+42m), geometric and material details of the updated FE model obtained from the iterative optimization algorithm. The primary outcomes of the

parametric analysis are:

- **Effect of the in-plane curvature of the deck.** The increment of the deck curvature causes the reduction of the natural frequencies of all the considered modes in the three FE classes. The eccentricity of the loads in the curved deck causes an additional torsion, which maximizes the inertial effects and reduces the natural frequencies. The inertial effect due to the deck curvature is partially compensated by the inclined tower, lessening eccentricity. Accordingly, the natural frequencies in the FE element models without and with the stay-cables reduce between the straight to the curved deck. On average, the percentage differences between natural frequencies are more significant in the torsional modes. This aspect proves that the additional inertial effects due to the load eccentricity are the leading cause of the frequency reduction associated with the torsional modes.
- **Effect of the stay-cables arrangement.** The adoption of stay-cables arranged in two symmetric planes should reduce the torsional effects on the deck. The difference between the linear structures in the second and third FE classes are minor. The double arrangement of the stay cables reduces the torsional response of the deck, leading to an increment of the torsional modes' natural frequency due to the higher torsional stiffness. However, the double curtain of stay cables causes a reduction of the natural frequency of the vertical bending modes due to the spatial eccentricity of the stay cables in the double-plane configuration, which causes an additional inertial effect on the vertical bending response. Conversely, the effects of the double plane of stay-cables are almost uniform in the curved deck cases. The double arrangement enhances the torsional stiffness of the deck, manifesting in a frequency increment of the torsional and bending modes.
- **Effect of the torsional inertia of the tower.** An increment of the rotational inertia of the tower affects all modes, not just the ones with a prevalent tower deformation. Still, the effects of the increased inertia are predominant in the torsional mode of the tower. The frequency increment is almost linearly proportional to the multiplication factors of the torsional inertia in the considered range of variation.

Future research efforts will aim to assess the Porto Marghera bridge's seismic performance and the parametric analysis of the effects of different design choices on the seismic response [41, 42, 43, 44, 45, 46, 47]. Additionally the authors will attempt to investigate the effect of the design choices on the in-plane lateral vibration of curved cable-stayed bridges [48].

Acknowledgements

The authors would like to thank the technical personnel (M. Antico and M. Cucchi) of the VIBLAB Laboratory of Vibrations and Dynamic Monitoring of Structures, Polytechnic of Milan, for the valuable help in conducting the field tests. Moreover, the collaboration of Dr. Fulvio Busatta (University of Cape Town) in implementing the first Finite Element Model and of Prof. Airong Chen (Tongji University) in performing a Risk Analysis of the Bridge are highly acknowledged. This work was supported by the National Natural Science Foundation of China [grant No. 51778148].

Disclosure statement

No potential competing interest was reported by the authors.

Funding

The authors gratefully acknowledge the financial support from the National Natural Science Foundation of China (Grant No. 51778148).

References

[1] M. Virlogeux, "Recent evolution of cable-stayed bridges," *Engineering structures*, vol. 21, no. 8, pp. 737–755, 1999.

[2] J. C. Wilson and T. Liu, "Ambient vibration measurements on a cable-stayed bridge," *Earthquake engineering & structural dynamics*, vol. 20, no. 8, pp. 723–747, 1991.

[3] A. Astaneh-Asl and R. G. Black, "Seismic and structural engineering of a curved cable-stayed bridge," *Journal of Bridge Engineering*, vol. 6, no. 6, pp. 439–450, 2001.

[4] Y.-C. Ni, Q.-W. Zhang, and J.-F. Liu, "Dynamic property evaluation of a long-span cable-stayed bridge (sutong bridge) by a bayesian method," *International Journal of Structural Stability and Dynamics*, vol. 19, no. 01, p. 1940010, 2019.

[5] C. Gentile and E. Siviero, "Dynamic characteristics of the new curved cable-stayed bridge in porto marghera (venice, italy) from ambient vibration measurements," in *IMAC-XXV*, pp. 1–10, 2007.

[6] M. De Miranda, A. De Palma, and A. Zanchettin, ""ponte del mare": Conceptual design and realization of a long span cable-stayed footbridge in pescara, italy," *Structural engineering international*, vol. 20, no. 1, pp. 21–25, 2010.

[7] B. Briseghella, E. Siviero, C. Lan, E. Mazzarolo, and T. Zordan, "Safety monitoring of the cable stayed bridge in the commercial harbor of venice, italy," in *Bridge Maintenance, Safety, Management and Life-Cycle Optimization: Proceedings of the Fifth International IABMAS Conference, Philadelphia, USA, 11-15 July 2010*, p. 379, CRC Press, 2010.

[8] Y. Deger, R. Cantieni, and C. de Smet, "Finite element model optimization of the new rhine bridge based on ambient vibration testing," *Balkema Publishers(Netherlands),*, pp. 817–822, 1996.

[9] J. M. Brownjohn and P.-Q. Xia, "Dynamic assessment of curved cable-stayed bridge by model updating," *Journal of structural engineering*, vol. 126, no. 2, pp. 252–260, 2000.

[10] C. Gentile and F. Martinez Y Cabrera, "Dynamic performance of twin curved cable-stayed bridges," *Earthquake engineering & structural dynamics*, vol. 33, no. 1, pp. 15–34, 2004.

[11] D. M. Siringoringo and Y. Fujino, "Dynamic characteristics of a curved cable-stayed bridge identified from strong motion records," *Engineering Structures*, vol. 29, no. 8, pp. 2001–2017, 2007.

[12] A. B. Halpern and D. P. Billington, "Eminent structural engineer: Michel virlogeux–structural artist of modern french bridges," *Structural Engineering International*, vol. 23, no. 3, pp. 350–353, 2013.

[13] K.-S. Kim and B.-I. Lee, "Current trends in concrete cable stayed bridge," *Magazine of the Korea Concrete Institute*, vol. 24, no. 2, pp. 10–15, 2012.

[14] O. S. Bursi, A. Kumar, G. Abbiati, and R. Ceravolo, "Identification, model updating, and validation of a steel twin deck curved cable-stayed footbridge," *Computer-Aided Civil and Infrastructure Engineering*, vol. 29, no. 9, pp. 703–722, 2014.

[15] W. E. Daniell and J. H. Macdonald, "Improved finite element modelling of a cable-stayed bridge through systematic manual tuning," *Engineering Structures*, vol. 29, no. 3, pp. 358–371, 2007.

[16] Q. Wen, X. Hua, Z. Chen, Y. Yang, and H. Niu, "Control of human-induced vibrations of a curved cable-stayed bridge: design, implementation, and field validation," *Journal of Bridge Engineering*, vol. 21, no. 7, p. 04016028, 2016.
[17] E. Zhang, D. Shan, S. Guo, J. Ren, and Q. Li, "Influence of curvature radius on static and dynamic characteristics of curved cable-stayed bridge," in *IABSE Symposium: Engineering the Future, Vancouver, Canada, 21-23 September 2017*, pp. 793–800, 2017.
[18] A. M. Martins, L. M. Simões, and J. H. Negrão, "Optimization of cable-stayed bridges: A literature survey," *Advances in Engineering Software*, vol. 149, p. 102829, 2020.
[19] A. Bonelli, O. Bursi, R. Ceravolo, S. Santini, N. Tondini, and A. Zasso, "Dynamic identification and structural health monitoring of a twin deck curved cable-stayed footbridge: the "ponte del mare" of pescara in italy," in *Proceedings of the 5th European Workshop on Structural Health Monitoring*, pp. 370–375, Sorrento, Italy, 2010.
[20] M. Friswell and J. E. Mottershead, *Finite element model updating in structural dynamics*, vol. 38. Springer Science & Business Media, 1995.
[21] A. Teughels, G. De Roeck, and J. A. Suykens, "Global optimization by coupled local minimizers and its application to fe model updating," *Computers & structures*, vol. 81, no. 24-25, pp. 2337–2351, 2003.
[22] R. Brincker, L. Zhang, and P. Andersen, "Modal identification from ambient responses using frequency domain decomposition," in *Proc. of the 18*th*International Modal Analysis Conference (IMAC), San Antonio, Texas*, 2000.
[23] T. Zordan, B. Briseghella, and T. Liu, "Finite element model updating of a tied-arch bridge using douglas-reid method and rosenbrock optimization algorithm," *Journal of Traffic and Transportation Engineering (English Edition)*, vol. 1, no. 4, pp. 280–292, 2014.
[24] S. Sehgal and H. Kumar, "Structural dynamic model updating techniques: a state of the art review," *Archives of Computational Methods in Engineering*, vol. 23, no. 3, pp. 515–533, 2016.
[25] F. Ferreira and L. Simões, "Least cost design of curved cable-stayed footbridges with control devices," in *Structures*, vol. 19, pp. 68–83, Elsevier, 2019.
[26] M. Bhagwat, S. Sasmal, B. Novak, and A. Upadhyay, "Dynamic performance evaluation of straight and curved cable-stayed bridges," *Bridge Structures*, vol. 5, no. 2-3, pp. 87–95, 2009.
[27] K. Takenouchi, "Single pylons for curved cable-stayed bridges," *Structural engineering international*, vol. 8, no. 4, pp. 269–272, 1998.
[28] Z. Shi, H. Hu, and J. Li, "Axis optimisation of arch-shaped pylons for high-speed railway cable-stayed bridges," *Engineering Structures*, vol. 227, p. 111424, 2021.
[29] M. De Miranda and E. Gnecchi-Ruscone, "Construction of the cable-stayed bridge in the commercial port of venice, italy," *Structural Engineering International*, vol. 20, no. 1, pp. 13–17, 2010.
[30] I. Talebinejad, C. Fischer, and F. Ansari, "Numerical evaluation of vibration-based methods for damage assessment of cable-stayed bridges," *Computer-Aided Civil and Infrastructure Engineering*, vol. 26, no. 3, pp. 239–251, 2011.
[31] D.-H. Yang, T.-H. Yi, H.-N. Li, and Y.-F. Zhang, "Monitoring and analysis of thermal effect on tower displacement in cable-stayed bridge," *Measurement*, vol. 115, pp. 249–257, 2018.
[32] J. S. Bendat, "Spectral techniques for nonlinear system analysis and identification," *Shock and Vibration*, vol. 1, no. 1, pp. 21–31, 1993.
[33] R. Allemang and D. L. Brown, "A correlation coefficient for modal vector analysis," 1982.
[34] Z.-D. Xu and Z. Wu, "Simulation of the effect of temperature variation on damage detection in a long-span cable-stayed bridge," *Structural Health Monitoring*, vol. 6, no. 3, pp. 177–189, 2007.
[35] Y. L. Xu and H. Zhou, "Damping cable vibration for a cable-stayed bridge using adjustable fluid dampers," *Journal of sound and vibration*, vol. 306, no. 1-2, pp. 349–360, 2007.
[36] A. R. Conn, N. I. Gould, and P. L. Toint, *Trust region methods*. SIAM, 2000.
[37] G. Fa, L. He, L. Fenu, E. Mazzarolo, B. Briseghella, and T. Zordan, "Comparison of direct and iterative methods for model updating of a curved cable-stayed bridge using experimental modal data," in *Proceedings of the IABSE Conference, Guangzhou, China*, pp. 8–11, 2016.
[38] S.-W. Kim, B.-G. Jeon, N.-S. Kim, and J.-C. Park, "Vision-based monitoring system for evaluating cable tensile forces on a cable-stayed bridge," *Structural Health Monitoring*, vol. 12, no. 5-6, pp. 440–456, 2013.
[39] D. Jana and S. Nagarajaiah, "Computer vision-based real-time cable tension estimation in dubrovnik cable-stayed bridge using moving handheld video camera," *Structural Control and Health Monitoring*, vol. 28, no. 5, p. e2713, 2021.
[40] S.-S. Jin, S. Jeong, S.-H. Sim, D.-W. Seo, and Y.-S. Park, "Fully automated peak-picking method for an autonomous stay-cable monitoring system in cable-stayed bridges," *Automation in Construction*, vol. 126, p. 103628, 2021.
[41] Y. Pang, X. Wu, G. Shen, and W. Yuan, "Seismic fragility analysis of cable-stayed bridges considering different sources of uncertainties," *Journal of Bridge Engineering*, vol. 19, no. 4, p. 04013015, 2014.
[42] J. Zhong, J.-S. Jeon, W. Yuan, and R. DesRoches, "Impact of spatial variability parameters on seismic fragilities of a cable-stayed bridge subjected to differential support motions," *Journal of Bridge Engineering*, vol. 22, no. 6, p. 04017013, 2017.
[43] L. Li, S. Hu, and L. Wang, "Seismic fragility assessment of a multi-span cable-stayed bridge with tall piers," *Bulletin of Earthquake Engineering*, vol. 15, no. 9, pp. 3727–3745, 2017.
[44] B. Wei, Z. Hu, X. He, and L. Jiang, "Evaluation of optimal ground motion intensity measures and seismic fragility analysis of a multi-pylon cable-stayed bridge with super-high piers in mountainous areas," *Soil Dynamics and Earthquake Engineering*, vol. 129, p. 105945, 2020.
[45] J. Yi and J. Li, "Modelling of stay cables with large earthquake-induced force variations in cable-stayed bridges," in *Structures*, vol. 33, pp. 627–636, Elsevier, 2021.
[46] K. Lin, Y.-L. Xu, X. Lu, Z. Guan, and J. Li, "Digital twin-based collapse fragility assessment of a long-span cable-stayed bridge under strong earthquakes," *Automation in Construction*, vol. 123, p. 103547, 2021.
[47] W. Xie and L. Sun, "Experimental and numerical investigations on transverse seismic responses of soil-cable-stayed-bridge system subjected to transverse near-fault ground motions," *Engineering Structures*, vol. 226, p. 111361, 2021.
[48] X. Su, H. Kang, J. Chen, T. Guo, C. Sun, and Y. Zhao, "Experimental study on in-plane nonlinear vibrations of the cable-stayed bridge," *Nonlinear Dynamics*, vol. 98, no. 2, pp. 1247–1266, 2019.

Conflict of Interest and Authorship Conformation

- All authors have participated in (a) conception and design, or analysis and interpretation of the data; (b) drafting the article or revising it critically for important intellectual content; and (c) approval of the final version.
- This manuscript has not been submitted to, nor is under review at, another journal or other publishing venue.
- The authors have no affiliation with any organization with a direct or indirect financial interest in the subject matter discussed in the manuscript

Author's name	Affiliation
BRUNO BRISEGHELLA	Sustainable and Innovative Bridge Engineering Research Center, College of Civil Engineering, Fuzhou University, China
GUANZHE FA	Sustainable and Innovative Bridge Engineering Research Center, College of Civil Engineering, Fuzhou University, China
ANGELO ALOISIO	Department of Civil, Construction-Architectural and Environmental Engineering, University of L'Aquila, Italy
DAG PASCA	Norsk Treteknisk Institutt (Norwegian Institute of Wood Technology), Børrestuveien 3, 0373 Oslo, Norway.
LEQIA HE	Sustainable and Innovative Bridge Engineering Research Center, College of Civil Engineering, Fuzhou University, China
LUIGI FENU	Department of Civil and Environmental Engineering and Architecture, University of Cagliari, Cagliari, Italy.
CARMELO GENTILE	Department of Architecture, Built environment and Construction engineering (DABC), Politecnico di Milano, Piazza Leonardo da Vinci 32, 20133 Milan Italy.